

This discussion paper is/has been under review for the journal Hydrology and Earth System Sciences (HESS). Please refer to the corresponding final paper in HESS if available.

Consistency between hydrological model, large aperture scintillometer and remote sensing based evapotranspiration estimates for a heterogeneous catchment

B. Samain¹, G. W. H. Simons², M. P. Voogt², W. Defloor³, N.-J. Bink⁴, and V. R. N. Pauwels¹

¹Laboratory of Hydrology and Water Management, Ghent University, Ghent, Belgium

²WaterWatch, Wageningen, The Netherlands

³Flemish Environmental Agency – Department Operational Water Management, Brussels, Belgium

⁴Wittich and Visser, Rijswijk, The Netherlands

Received: 17 November 2011 – Accepted: 23 November 2011 – Published: 9 December 2011

Correspondence to: B. Samain (bruno.samain@ugent.be)

Published by Copernicus Publications on behalf of the European Geosciences Union.

HESSD

8, 10863–10894, 2011

Consistency between hydrological model, LAS and remote sensing

B. Samain et al.

Discussion Paper | Discussion Paper

Discussion Paper | Discussion Paper

Title Page

Abstract

Introduction

Conclusions

References

Tables

Figures

◀

▶

Back

Close

Full Screen / Esc

Printer-friendly Version

Interactive Discussion



Abstract

The catchment averaged actual evapotranspiration rate is a hydrologic model variable that is difficult to quantify. Evapotranspiration rates can – up till present – not be continuously observed at the catchment scale.

5 The objective of this paper is to estimate the evapotranspiration rates (or its energy equivalent, the latent heat fluxes LE) for a heterogeneous catchment of 102.3 km^2 in Belgium using three fundamentally different algorithms.

One possible manner to observe this variable could be the continuous measurement of sensible heat fluxes (H) across large distances (in the order of kilometers) using a
10 Large Aperture Scintillometer (LAS), and inverting these observations into evapotranspiration rates. Latent heat fluxes are obtained through the energy balance equation using a series of sensible heat fluxes (H) measured with a LAS over a distance of 9.5 km in the catchment, and point measurements of net radiation (R_n) and ground heat flux (G) upscaled to catchment average through the use of TOPLATS, a physically
15 based land surface model.

The resulting LE-values are then validated by comparing them to results from the remote sensing based surface energy balance algorithm ETLook and the land surface model. Firstly, it is demonstrated that ETLook is able to estimate the energy balance terms for daily time steps at the point scale and at the catchment scale. Secondly,
20 consistency between daily evapotranspiration rates from ETLook, TOPLATS and LAS is shown.

As such, ETLook provides the opportunity to estimate continuous series of the energy balance terms of a large area for daily time steps and can thus e.g. be used as a validation tool for LAS-measurements, whereas LAS is able to estimate the latent heat fluxes (evapotranspiration rates) for a large and heterogeneous catchment at an hourly time step which can be used for the forcing or validation of hydrologic models.
25

Evapotranspiration (ET) estimates are needed for a wide range of problems in hydrology, agronomy, forestry and land management, and water resources planning, such as water balance computation, river flow forecasting, ecosystem modeling, etc. Due to complex interactions amongst the components of the land-plant-atmosphere system, evapotranspiration is perhaps the most difficult of all the components of the hydrologic cycle to assess (Xu and Singh, 2005).

Most methods for the estimation of evapotranspiration rates are point-scale approaches. Estimates at large spatial scales can be obtained using remote sensing and spatially distributed hydrological models. For large scale assessment of ET, extended networks of (field) sensors have a large potential for ET estimation. However, typically, regional to continental scale information on ET is obtained with the application of earth observation techniques, although thermal and optical techniques require clear sky imagery (Verstraeten et al., 2008), which limits these techniques for the continuous observation of ET.

The scintillation method is an attractive method for a routinely observation of the surface fluxes across large distances (Meijninger et al., 2002). For evapotranspiration (or its energy equivalent, latent heat flux LE) measurements, scintillometers operating at radio wave lengths are best suited, but for a variety of reasons (expensive technology, complexity, absorption effects, and required licenses), these are yet not commercially available (Meijninger et al., 2006). At present, optical scintillometers are more widely used, but they can only estimate the sensible heat flux across a large distance.

A number of studies have already focused on estimation of evapotranspiration rates (or LE) from sensible heat flux measurements acquired from LAS-data. In all of these studies, the latent heat flux is always estimated as the rest-term of the energy balance ($LE = R_n - G - H$). So, the estimation of a representative value for the available energy ($AE = R_n - G$) is always crucial for the accuracy of the retrieved values of LE.

Consistency between hydrological model, LAS and remote sensing

B. Samain et al.

[Title Page](#)

[Abstract](#)

[Introduction](#)

[Conclusions](#)

[References](#)

[Tables](#)

[Figures](#)



[Back](#)

[Close](#)

[Full Screen / Esc](#)

[Printer-friendly Version](#)

[Interactive Discussion](#)

Consistency between hydrological model, LAS and remote sensing

B. Samain et al.

For short scintillometer paths over a homogeneous surface, Pauwels and Samson (2006) and Savage (2009) showed that the latent heat flux as rest-term of the energy balance where H is measured by a scintillometer and R_n and G are measured at a point location along the scintillometer path, resulted in a good agreement between the LAS-derived latent heat fluxes and LE as measured with Bowen Ratio Energy Balance (BREB) and Eddy Covariance (EC) – stations along the path. The same method was used for a larger and more heterogeneous areas by Ezzahar and Chehbouni (2009) and Bai et al. (2009) who used the H from a scintillometer measuring over a distance of about 1 and 2.5 km, respectively, combined with point measurements of R_n and G within the scintillometer path to calculate the area averaged sensible heat flux. Hemakumara et al. (2003) estimated the latent heat flux on a daily basis (24 h) from LAS-measured H -fluxes over an almost 2 km path length with mixed land cover and point-measurements of R_n . As LE was estimated on a daily basis, the soil heat storage was assumed to be minimal, and $LE_{24\text{h}}$ has been calculated from $R_{n,24\text{h}}$ and $H_{24\text{h}}$ with promising results in a comparison with results from a remote sensing based surface energy balance algorithm. Guyot et al. (2009) calculated the spatially averaged latent heat flux for a small (12 km^2), heterogeneous catchment in West Africa (Northern Benin) as the residual term of the energy balance equation where H was measured with a scintillometer over the catchment, using point measurements of R_n which were shown to be representative for the heterogeneous catchment in wet conditions, and aggregated values of G which were obtained as a simple average of local G -estimations based on soil temperature measurements at three different locations within the catchment. Ezzahar et al. (2009) derived the area-averaged latent heat flux as the residual term of the energy balance equation through the combination of the LAS measurements over a 3.2 km slanted, heterogeneous path, and an aggregation scheme to derive area-average available energy based on the local measurements of the surface temperature, the albedo and the incoming solar radiation, all measured over the three different vegetation types. From all of these studies, it was concluded that a LAS is an adapted device to estimate the actual evapotranspiration through an

Title Page

Abstract

Introduction

Conclusion:

References

Tables

Figures



Bac

Close

Full Screen / Esc

[Printer-friendly Version](#)

Interactive Discussion

Consistency between hydrological model, LAS and remote sensing

B. Samain et al.

[Title Page](#)

[Abstract](#)

[Introduction](#)

[Conclusions](#)

[References](#)

[Tables](#)

[Figures](#)



[Back](#)

[Close](#)

[Full Screen / Esc](#)

[Printer-friendly Version](#)

[Interactive Discussion](#)

Consistency between hydrological model, LAS and remote sensing

B. Samain et al.

[Title Page](#)

[Abstract](#)

[Introduction](#)

[Conclusions](#)

[References](#)

[Tables](#)

[Figures](#)



[Back](#)

[Close](#)

[Full Screen / Esc](#)

[Printer-friendly Version](#)

[Interactive Discussion](#)

remote sensing data is a good validation tool for flux measurements over a large and heterogeneous area (as can be done with a scintillometer), the used remote sensing techniques are restricted by cloud coverage (Hemakumara et al., 2003) and only the instantaneous moments of satellite overpass can be validated (Kleissl et al., 2009a).

Recently, Samain et al. (2011a) used a Large Aperture Scintillometer (LAS), installed across a distance of 9.5 km, to estimate the spatially averaged sensible heat flux for the 102.3 km² heterogeneous Bellebeek catchment in Belgium. Through the use of a spatially distributed land surface model and a footprint analysis, they showed that the measurements of this LAS in unstable (daytime) conditions are representative for the entire catchment. In a next step, different algorithms have been evaluated to produce a continuous series (including stable conditions) of H from the LAS data (Samain et al., 2011b).

The main goal of this study is to explore the consistency for evapotranspiration estimates over a large, heterogeneous area between three fundamentally different techniques: the LAS-based values of actual evapotranspiration using LAS- H and the energy balance approach, the land surface model TOPLATS, and the remote sensing algorithm ETLook that is developed to calculate ET for lower temporal resolutions (daily time step).

A first objective of this paper is to make continuous series of hourly actual evapotranspiration rates for the Bellebeek catchment based on LAS measurements and the energy balance approach. This continuous catchment averaged actual ET-series can then, for example, be used as model forcing for rainfall-runoff models or for the validation of land surface and weather prediction models. Therefore, the continuous series of H based on the LAS-data is used in combination with areally representative values of available energy ($\langle AE \rangle = \langle R_n - G \rangle$). The estimates of $\langle AE \rangle$ are based on local measurements of R_n and G which have been validated and upscaled for the heterogeneous catchment through the use of the calibrated spatially distributed physically based land surface model as described in and applied by Samain et al. (2011a). This results in an operationally applicable technique for the estimation of catchment averaged actual

evapotranspiration rates through the combination of only three measurements (H from LAS, and locally measured, but upscaled values for $\langle AE \rangle = \langle R_n - G \rangle$).

The second objective is to check the consistency of the LAS-derived series of evapotranspiration rates on a daily basis for a period of six months through comparison with the results of ETLook, an algorithm based on remote sensing data to compute continuous daily evapotranspiration rates for large areas. Before checking the consistency between LAS- and ETLook-results, the performance of ETLook is checked by comparing ETLook-results to point-measurements and to catchment averaged fluxes as modeled with the land surface model.

10 2 Site and data description

2.1 Site description

The study was performed in the Dender catchment in Belgium. Figure 1 shows the location of the catchment together with a Digital Elevation Model (DEM) of the area. A LAS was installed in the sub-catchment of the Bellebeek (102.3 km^2). The elevation in the sub-catchment ranges between 10 and 110 m. Soil texture is predominantly loam (74 %), and the land use is predominantly agriculture (63.6 %) and pasture (22.9 %). 15 8.6 % of the surface consists of urban land cover and the remaining area consists of forest (4.8 %) and open water (0.1 %).

2.2 Surface data sets

20 Figure 1 shows the location of the meteorological station used in this study. Continuous measurements of wind speed and wind direction at 10 m height, as well as precipitation rates, air pressure, and air and dew point temperature at a height of 2 m were available at a 10-min interval from the meteorological station of Liedekerke, situated near the outlet of the catchment. Further, net radiation data from a NR-Lite net radiometer (Kipp

Consistency between hydrological model, LAS and remote sensing

B. Samain et al.

[Title Page](#)

[Abstract](#)

[Introduction](#)

[Conclusions](#)

[References](#)

[Tables](#)

[Figures](#)

◀

▶

[Back](#)

[Close](#)

[Full Screen / Esc](#)

[Printer-friendly Version](#)

[Interactive Discussion](#)



Consistency between hydrological model, LAS and remote sensing

B. Samain et al.

[Title Page](#)[Abstract](#)[Introduction](#)[Conclusions](#)[References](#)[Tables](#)[Figures](#)[Back](#)[Close](#)[Full Screen / Esc](#)[Printer-friendly Version](#)[Interactive Discussion](#)

and Zonen, Delft, Netherlands) at 2 m height and ground heat flux observations from two HFP01 soil heat flux sensors (Hukseflux, Delft, Netherlands) at 5 cm depth were also available at this site.

From 15 April 2009, an Eddy Covariance (EC) installation was installed at 2 m above the surface of a grassland in Ternat approximately in the middle of the scintillometer-path. The EC station consists of a 3-D sonic anemometer (CSAT3, Campbell Scientific Ltd.), and a Krypton hygrometer (KH_2O , Campbell Scientific Ltd.). Raw data were sampled at a rate of 10 Hz. The half-hourly fluxes were calculated off-line using the TK2 software package (Mauder and Foken, 2004; Mauder et al., 2008). With the TK2-package, the fluxes were calculated after despiking, cross wind correction, planar fit correction, correction of oxygen cross sensitivity for the Krypton hygrometer, correction of spectral loss, and correction for density fluctuations (WPL-correction, Webb et al., 1980). In combination with this EC-station net radiation (NR-lite net radiometer – Kipp and Zonen, Delft, The Netherlands) at 2 m above the surface and soil heat flux (two HFP01SC soil heat flux sensors – Hukseflux, Delft, The Netherlands) just below the surface were registered at a 10 min interval and were averaged to one hour intervals.

2.3 Scintillometer data

2.3.1 Introduction

As described by Samain et al. (2011a), the scintillometer used in this experiment is a Large Aperture Scintillometer (LAS), type BLS2000 (Scintec AG, Tübingen, Germany). The transmitter is situated in Asse on a water tower at an elevation of 40 m above the surface. The receiver is installed in the church tower in Eizeringen at 15 m above the surface. The LAS is thus measuring over the sub-catchment of the Bellebeek along a 9.5 km path. This allows the beam to cross the basin well above the canopy, the small forests, the valley of the Bellebeek and its tributaries and roads and towns. According to Samain et al. (2011a), the effective height (z_{eff} , m) of the beam is 68 m, calculated following Hartogensis et al. (2003). The BLS2000 has an aperture

Consistency between hydrological model, LAS and remote sensing

B. Samain et al.

[Title Page](#)[Abstract](#)[Introduction](#)[Conclusions](#)[References](#)[Tables](#)[Figures](#)[◀](#)[▶](#)[Back](#)[Close](#)[Full Screen / Esc](#)[Printer-friendly Version](#)[Interactive Discussion](#)

size of 0.26 m, suitable for flux-measurements on a relatively large spatial scale (up to 10 km) without running into the problem of saturation of the LAS signal (Kohsieck et al., 2006). From the 1-min data of observed intensities, 1-min H -values are derived using the calculation procedure as explained in Samain et al. (2011a). As can be seen from this procedure, obtaining the sensible heat flux from a scintillometer measurement over a heterogeneous area requires the measurement of a number of additional parameters (Table 1): air temperature, air pressure, Bowen ratio, zero-plane displacement height, and friction velocity representative for the area under the LAS. As shown in Samain et al. (2011a), representative sensible heat fluxes for the heterogeneous catchment of the Bellebeek can be calculated from the LAS data at 68 m height in combination with the air temperature and air pressure from the meteorological station at Liedekerke, the zero-plane displacement height estimated as 0.7 m and the friction velocity calculated from the measured wind speed at the Liedekerke meteorological station. The 1-min values of H are then averaged per hour. Samain et al. (2011b) further describe the construction of an almost continuous series of hourly sensible heat fluxes using an operational algorithm based on the diurnal cycle of the refractive index structure parameter C_N^2 and by ignoring the humidity correction based on the Bowen ratio. This ignoring of the humidity correction has been shown to result in an increase of the completeness of the resulting H -series with only a marginal error in H . In this paper, the energy balance equation will be applied to calculate latent heat fluxes from these H -fluxes.

2.3.2 Available time series from LAS

The LAS in the Bellebeek catchment is operational since 21 February 2008. For the present study, data from six months (from 1 April 2009 through 30 September 2009) are used. Unfortunately, due to logging problems, no LAS-data were available for three periods within these six months: from 9 June 2009, through 2 July 2009, from 10 July 2009 through 14 July 2009, and from 16 September 2009 through 20 September 2009. For this six months period (4392 hourly time steps), no LAS data are available

for 755 time steps (or 17.2 % of the time steps). Using the algorithm for constructing a continuous time series of H from LAS as explained by Samain et al. (2011b), from the remaining 3637 time steps, a reliable estimate of H could be obtained for 3100 time steps, which is an availability of approximately 85 % of the available LAS-time steps.

- 5 The loss of 15 % of the data is because no reliable H could be calculated because of precipitation (7.2 %) or because no reliable hourly C_N^2 was obtained from LAS-data (1.3 %) or the algorithm could not be applied (6.3 %).

3 $\langle LE \rangle$ from LAS

A LAS provides the opportunity to provide surface fluxes of sensible heat across a distance of several kilometers and over a heterogeneous landscape. As shown by different authors, it is feasible to use the LAS for operationally estimating area-averaged $\langle LE \rangle$ as the residual term of the energy balance equation, providing estimates of area-average available energy ($\langle AE \rangle = \langle R_n - G \rangle$) are available. Samain et al. (2011a) have shown that the LAS measurements over a distance of 9.5 km and an effective height

15 of 68 m are representative for the entire catchment of 102.3 km^2 . To calculate representative values for $\langle LE \rangle$ from the energy-balance approach, representative values for the available energy $\langle AE \rangle$ are required. $\langle AE \rangle$ could be constructed by deploying a network of net radiometers (R_n) and soil heat flux plates (G) on the different land cover types and soil wetness conditions within the catchment. However, this approach is

20 practically not feasible. Not only because the considered catchment is very heterogeneous, which would require a large amount of point-measurements, but also because the surface heat fluxes do not only depend on the land cover type, but also on the soil moisture conditions, which can show a high spatial variability within the catchment (Samain et al., 2011a). So an aggregation scheme for $\langle AE \rangle$ -calculation based on only

25 point-measurements cannot be applied. The aggregation scheme based on local measurementes of surface temperature, albedo and solar radiation as proposed by Ezzahar et al. (2009) suffers from the same drawback, due to the high level of heterogeneity of

[Title Page](#)[Abstract](#)[Introduction](#)[Conclusions](#)[References](#)[Tables](#)[Figures](#)[◀](#)[▶](#)[Back](#)[Close](#)[Full Screen / Esc](#)[Printer-friendly Version](#)[Interactive Discussion](#)

Title Page	
Abstract	Introduction
Conclusions	References
Tables	Figures
◀	▶
◀	▶
Back	Close
Full Screen / Esc	
Printer-friendly Version	
Interactive Discussion	

the Bellebeek catchment. Therefore, for this study, the results of the calibrated land surface model as used by Samain et al. (2011a) for validation of the representativeness of $\langle H \rangle$ for the catchment will be used here to convert point-measured values of AE to area-averaged values for $\langle AE \rangle$.

5 3.1 The hydrologic model (TOPLATS)

As described more extensively in Samain et al. (2011a), the land-surface model used is the TOPMODEL-Based Land-Atmosphere Transfer Scheme (TOPLATS). It is a physically based, spatially distributed land surface model that for every pixel within the catchment, solves the surface energy balance equation through an iteration for the 10 soil surface temperature.

As listed in Table 1, the TOPLATS model for the Bellebeek catchment uses a digital elevation model, soil texture and land cover maps and continuous meteorological observations which are considered to be representative for and uniformly distributed over for the study area. In Samain et al. (2011a), the land surface model has been 15 calibrated and validated using discharge and energy balance terms at an hourly time step. A good correspondence between observed and modeled discharge showed the accuracy of the model at the catchment scale. The accuracy of the model at the point scale was illustrated by the ability to simulate net radiation and soil heat flux at the pixel where BREB (Bowen Ratio Energy Balance)-stations were located, and latent 20 and sensible heat flux from the source areas around the BREB-stations (Samain et al., 2011a).

The model has further been used to validate the LAS measurement of the sensible heat flux over a distance of 9.5 km with H as modeled within the footprint and within the catchment (102.3 km^2). For unstable conditions, it has been concluded that the LAS 25 measurements of the sensible heat flux are representative for the catchment (Samain et al., 2011a).

3.2 From point-measured AE to catchment averaged (AE)

Consistency between hydrological model, LAS and remote sensing

B. Samain et al.

The objective of this study is to obtain $\langle AE \rangle$ in an operational way. Using the energy balance approach, this requires operational estimates of catchment-representative values of the available energy (AE), which are acquired from point-measurements and model results. At the meteorological station of Liedekerke, net radiation ($R_{n,Liedekerke}$) and soil heat flux ($G_{Liedekerke}$) are continuously measured. From these data, point-values of AE can be calculated as $AE_{Liedekerke} = R_{n,Liedekerke} - G_{Liedekerke}$. As area-average observations of net radiation and soil heat flux are not available, the catchment averaged available energy as calculated with the TOPLATS-model for every pixel within the catchment ($\langle AE \rangle_{TOPLATS} = R_{n,TOPLATS} - G_{TOPLATS}$) is used to validate the local measurements of $AE_{Liedekerke}$ for the catchment. For the period from 1 January 2008 through 8 April 2011, the hourly values of $\langle AE \rangle_{TOPLATS}$ are compared to the ground-based measurements of $AE_{Liedekerke}$ in Fig. 2a. The mean monthly values of $AE_{Liedekerke}$ and $\langle AE \rangle_{TOPLATS}$ are given in Table 2. From this figure and table, it can be concluded that the point-measurements of AE overestimate the catchment averaged $\langle AE \rangle$. As the linear regression with a correlation coefficient R of 0.96 shows a good correspondence between both AE-values, but an overestimate of $\langle AE \rangle$ by the Liedekerke point-measurements (slope of 0.86), a simple regression could be applied for the conversion of $AE_{Liedekerke}$ to $\langle AE \rangle$ -values. Nevertheless, from regressions taken per month (Table 2), it seems that there is an annual pattern in the regression slopes. This can be explained by the fact that the point-measurements are taken on a grass field where vegetation does not change much throughout the year, while the model results are an average for the entire catchment where the vegetation is changing throughout the year as e.g. crops are sown, grow and harvested again, resulting in a different radiation budget. In order to take into account this dynamic character of the catchment, the parameters of the monthly regressions (Table 2) are used to convert the point measurements of $AE_{Liedekerke}$ into $\langle AE \rangle_{TOPLATS}$ -values, which can be considered as catchment averaged values of $\langle AE \rangle$. The converted values of $\langle AE \rangle$ from the point-measured

[Title Page](#)

[Abstract](#)

[Introduction](#)

[Conclusions](#)

[References](#)

[Tables](#)

[Figures](#)

◀

▶

◀

▶

[Back](#)

[Close](#)

[Full Screen / Esc](#)

[Printer-friendly Version](#)

[Interactive Discussion](#)

3.3 $\langle LE \rangle$ from $\langle AE \rangle$ and $\langle H \rangle$

- 5 As the point-measurements of $\text{AE}_{\text{Liedekerke}}$ can be considered as being operationally available because they are retrieved from a permanent meteorological station, the above regression approach would allow to continuously and operationally calculate catchment averaged values of $\langle \text{AE} \rangle$, which can be used for continuously calculating the catchment averaged latent heat flux $\langle \text{LE} \rangle$ using the energy balance equation and

10 values of $\langle H \rangle$ as retrieved from the LAS. For the hourly time steps where LAS-data are available and $\langle H \rangle$ could be calculated according to the principles explained by Samain et al. (2011b) in order to become a continuous series of $\langle H \rangle$ (stable and unstable conditions), $\langle \text{LE} \rangle$ is calculated as $\langle \text{AE} \rangle - \langle H \rangle$. These values of $\langle \text{LE} \rangle$ can then be validated by comparing them to results of the remote sensing model ETLook.

15 4 ⟨LE⟩ from ETLook

As explained earlier, it is infeasible to validate area-averaged values of $\langle LE \rangle$ for the heterogeneous Bellebeek catchment with a weighted average of ground-based LE-measurements. Therefore, the remote sensing-based algorithm ETLook is used to validate $\langle LE \rangle$ for a limited time period.

- ETLook is an algorithm developed by WaterWatch (Pelgrum et al., 2010) to compute evapotranspiration based on remote sensing data. ETLook has been developed in addition to the SEBAL model (Bastiaanssen et al., 1998). Being mainly driven by actual soil moisture instead of surface temperature, usage of ETLook avoids the limiting factors of models based on closure of the energy balance. These include poor suitability of the models in larger areas, where differences in surface temperature cannot

10875



be solely explained by differences in the surface energy balance. Also, ETLook does not rely on thermal infrared sensors sensitive to cloudy conditions, which is a particular advantage in regions with a temperate climate. The model has been tested for different climatological conditions and locations around the world (Pelgrum et al., 2010).

5 ETLook distributes incoming solar radiation over canopy and soil within a pixel based
 on satellite-derived Leaf Area Index (LAI) values. The Penman-Monteith equation is
 solved separately for vegetation and soil in order to split the evapotranspiration (ET)
 into transpiration (T) and evaporation (E):

$$T = \frac{\Delta(R_{n,canopy}) + \rho c_p \frac{\Delta_e}{r_{a,canopy}}}{\Delta + \gamma \left(1 + \frac{r_{canopy}}{r_{a,canopy}} \right)} \quad (1)$$

$$E = \frac{\Delta(R_{n,soil} - G) + \rho c_p \frac{\Delta_e}{r_{a,soil}}}{\Delta + \gamma \left(1 + \frac{r_{soil}}{r_{a,soil}} \right)} \quad (2)$$

where Δ is the slope of the saturation vapour pressure curve (mbar K^{-1}), Δ_e is the vapor pressure deficit (mbar), ρ is the air density (kg m^{-3}), c_p is the specific heat of dry air ($\text{J kg}^{-1} \text{K}^{-1}$), γ is the psychrometric constant (mbar K^{-1}), G is the soil heat flux (W m^{-2}), $R_{n,\text{canopy}}$ and $R_{n,\text{soil}}$ (W m^{-2}) are the net radiation for canopy and soil, respectively, r_{canopy} and r_{soil} (s m^{-1}) are the canopy and soil resistance, respectively, and $r_{a,\text{canopy}}$ and $r_{a,\text{soil}}$ (s m^{-1}) are the aerodynamic canopy and soil resistance, respectively. The aerodynamic canopy and soil resistance, $r_{a,\text{canopy}}$ and $r_{a,\text{soil}}$, are a function of wind speed and surface roughness. The latter is computed based on land cover information acquired from the Corine dataset (European Environment Agency, 2006), and is corrected for satellite-derived NDVI values for every day of the modeling period. The soil resistance r_{soil} is a function of the soil moisture content in the top soil, which can be derived from remote sensing observations (such as AMSR-E microwave measurements). The canopy resistance r_{canopy} is a function of the LAI and four dimensionless



Consistency between hydrological model, LAS and remote sensing

B. Samain et al.

[Title Page](#)[Abstract](#)[Introduction](#)[Conclusions](#)[References](#)[Tables](#)[Figures](#)[Back](#)[Close](#)[Full Screen / Esc](#)[Printer-friendly Version](#)[Interactive Discussion](#)

on different input data as compared to the LAS-approach. As such, ETLook provides a good validation tool for LAS-derived fluxes.

5 Results and discussion

5.1 Performance of ETLook

- 5 Before evaluating the consistency between LAS-derived $\langle LE \rangle$ and ETLook-derived $\langle LE \rangle$, the output of the ETLook algorithm is validated on the point scale and on the catchment scale. Therefore, ETLook-results are compared, respectively to measurements of the Eddy Covariance station in Ternat and to TOPLATS model results of the catchment.
- 10 For the validation at the point scale, the calculated fluxes from the pixel where the EC-station is situated are extracted from the ETLook grids and compared to daily averages of the EC-measurements. A valid value for a daily average is calculated when more than 12 hourly data (out of 24 h) are available. Scatter plots of this comparison for daily available energy ($R_n - G$), H and LE are shown in Fig. 3a–c, respectively.
- 15 As can be seen from Fig. 3a, ETLook succeeds rather well in estimating the available energy at the point-scale (slope = 0.88 and determination coefficient $R = 0.935$). The ETLook estimated sensible and latent heat fluxes do reasonably agree with the EC-measurements. However, there is some mismatch ($R = 0.65$ and 0.61 for H and LE , respectively) which e.g. can be due to a footprint issue, because the source area of
- 20 the EC-measurement exceeds the 30 m resolution of ETLook (Samain et al., 2011a), or due to missing data throughout the day which influences the daily averages of the fluxes. Apart from these explanations, it is probably mainly caused by the energy balance closure problem of the EC-technique. From the mean values of H and LE , it can be seen that ETLook estimates both fluxes to be higher than measured with the
- 25 EC-equipment. On the extra scatterplot in Fig. 3a, the sum of H and LE as measured with the EC-sations is plotted against the available energy measured at the Ternat

Title Page	
Abstract	Introduction
Conclusions	References
Tables	Figures
◀	▶
◀	▶
Back	Close
Full Screen / Esc	
Printer-friendly Version	
Interactive Discussion	

Consistency between hydrological model, LAS and remote sensing

B. Samain et al.

[Title Page](#)

[Abstract](#)

[Introduction](#)

[Conclusions](#)

[References](#)

[Tables](#)

[Figures](#)

[◀](#)

[▶](#)

[◀](#)

[▶](#)

[Back](#)

[Close](#)

[Full Screen / Esc](#)

[Printer-friendly Version](#)

[Interactive Discussion](#)



station. From the mean values and the slope of 0.8, it is clear that for most of the daily time steps, $H + LE$ is less than $R_n - G$, which means that the measurements from the EC-station show an unclosed energy-balance, a problem that has been described extensively. According to Foken (2008), the energy balance closure problem of EC-

measurements is not a problem of measurement errors or storage terms, but a scale problem as EC equipment is not able to measure the exchange processes on the larger scale and as such, does not measure large scale fluxes that also need to be accounted for in the energy balance at the point scale.

At the catchment scale, the average of the fluxes calculated by ETLook for all pixels within the catchment are compared to the catchment averaged fluxes as calculated by TOPLATS and averaged to a daily time step. Scatterplots for $\langle AE \rangle$, $\langle LE \rangle$ and $\langle H \rangle$ for daily timesteps where all data are available are shown in Fig. 3d–f, respectively. The daily time series as well as a plot of the cumulative fluxes for the available time steps in the considered 6 months period is shown in Fig. 4. In general, a small bias and small RMSE values for all the energy balance terms have been obtained. Furthermore, the high R -values and the fact that all slopes have a value of almost 0.9 indicate that ETLook and TOPLATS have comparable results for $\langle AE \rangle$, $\langle H \rangle$ and $\langle LE \rangle$ and as such ETLook performs equally well as the spatially distributed hydrological model for the estimation of the catchment averaged fluxes on a daily basis.

20 5.2 Consistency between LAS, ETLook and TOPLATS

As ETLook is able to estimate the energy balance terms at the point scale and at the catchment scale, it can be used to validate the latent heat flux (or evapotranspiration rates) as estimated from the LAS. Samain et al. (2011a) have shown that the sensible heat flux estimates from the LAS in unstable conditions are representative for the catchment.

To check the consistency between LAS-and remote sensing-based fluxes, the daily averages of the measured sensible heat flux by the LAS, the used values of available energy to convert LAS- H into LE-values and the resulting latent heat flux from the

energy balance equation are compared to the catchment-average of these daily fluxes ($\langle AE \rangle$, $\langle H \rangle$ and $\langle LE \rangle$) calculated by ETLook. Scatterplots for all these components of the energy balance on the catchment scale are presented in Fig. 5a–c, respectively, while the time series are shown in Fig. 4.

5 The scatterplot and timeseries of $\langle AE \rangle$ reveal that the available energy for the catchment as estimated from the Liedekerke point-measurements but upscaled to the catchment through the use of the hydrologic model, shows good correspondence with the catchment available energy as calculated by ETLook.

As for the catchment averaged sensible $\langle H \rangle$ and latent $\langle LE \rangle$ heat flux, the scatters
10 show some larger differences. As for this analysis, valid daily averages of the LAS-
derived fluxes are considered where at least for 12 h out of 24 data are available to
calculate $\langle H \rangle$ and $\langle LE \rangle$, the differences can maybe partly be explained by this calcula-
tion procedure for the daily averages. As Samain et al. (2011b) states that the daily
15 average of H derived from LAS-data can be largely influenced by a wrong estimate for
 H during some hours of the day (Samain et al., 2011b showed this for the assumption
of H being 0 W m^{-2} during stable conditions instead of a negative value as measured
by the LAS), daily estimates of $\langle H \rangle$ and $\langle LE \rangle$ for days where less than 24 hourly data are
available from LAS can show some difference in comparison with the daily averages
as estimated by ETLook. Therefore, in a second analysis, only the days are consid-
20 ered where the daily averages of $\langle H \rangle$ and $\langle LE \rangle$ are based on 24 valid hourly values from
LAS. For these days, the scatterplots of the daily averaged fluxes are given in Fig. 5d–f.
From these scatterplots, it is clear that less daily data are available for comparison, but
that the estimated fluxes of $\langle H \rangle$ and $\langle LE \rangle$ match much better. The fluxes calculated with
ETLook and the estimated fluxes from LAS-data correlate better and are closer to the
25 expected 1 : 1 relation. From this comparison it can also be seen that LAS estimates
the daily average of $\langle H \rangle$ on average slightly higher than ETLook and as both estimates
of $\langle LE \rangle$ are based on the energy balance equation, it is clear that the LAS-derived daily
 $\langle LE \rangle$ -fluxes are on average slightly lower than estimated by ETLook.

Consistency between hydrological model, LAS and remote sensing

B. Samain et al.

[Title Page](#)

[Abstract](#)

[Introduction](#)

[Conclusions](#)

[References](#)

[Tables](#)

[Figures](#)



[Back](#)

[Close](#)

[Full Screen / Esc](#)

[Printer-friendly Version](#)

[Interactive Discussion](#)

Consistency between hydrological model, LAS and remote sensing

B. Samain et al.

As the main purpose of the LAS-installation is to provide estimates of catchment averaged actual evapotranspiration rates as input for a flood forecasting model for the Bellebeek catchment, the focus is on the resulting evapotranspiration rates as they will play an important role in the water balance and thus on the output of the flood forecasting model. In order to assess the influence on the water balance, for the overlapping days of the considered techniques (based on 24 hourly values), daily evapotranspiration rates (in mm) are calculated from latent heat fluxes (in W m^{-2}) and summed per 10-day period (Table 3). Overall, the evapotranspiration rates from the three different techniques resemble very well. Looking into detail at the table shows that the slightly lower estimates for $\langle \text{LE} \rangle$ as derived from LAS-data in comparison with ETLook appear in April and September. For those months, the resemblance between ETLook- and TOPLATS-results is slightly better. For the other months there is no clear over- or underestimation of the 10-day evapotranspiration estimates by any of the three techniques used.

Samain et al. (2011a) mentioned an underestimate of $\langle H \rangle$ as measured with the LAS compared to the TOPLATS results. Different possible explanations for this underestimation of $\langle H \rangle$ have been mentioned, such as the saturation effect, flux divergence and/or uncertainty of the stability functions. This underestimate of $\langle H \rangle$ would result in an overestimate of LAS-derived $\langle \text{LE} \rangle$ compared to TOPLATS. However, from the 10-day evapotranspiration rates, this overestimate of $\langle \text{LE} \rangle$ by LAS compared to TOPLATS is not clear for the considered period in this study. Probably a better judgement of stable and unstable conditions for the LAS (as explained by Samain et al., 2011b) or the model parameters for TOPLATS are an explanation for the better agreement between TOPLATS and LAS for the considered period.

[Title Page](#)[Abstract](#)[Introduction](#)[Conclusions](#)[References](#)[Tables](#)[Figures](#)[Back](#)[Close](#)[Full Screen / Esc](#)[Printer-friendly Version](#)[Interactive Discussion](#)

6 Summary and conclusions

In this paper, daily estimates of the evapotranspiration rates for a heterogeneous catchment of 102.3 km^2 from three different techniques have been made and intercompared.

Firstly, the catchment averaged evapotranspiration rates are estimated from the energy balance approach based on LAS-measurements of H over a 9.5 km path within the catchment and estimates of the available energy for the catchment. Operational estimates of the catchment available energy are calculated from point measurements of R_n and G in the catchment and adjusted to the catchment scale through the use of the calibrated land surface model TOPLATS.

Secondly, ETLook is introduced as a remote sensing tool to estimate continuous series of the energy balance terms for large areas and for high temporal resolutions (up to daily time step) without the restriction of cloud free conditions. As such, ETLook provides the opportunity to validate large-scale estimates of the sensible and latent heat flux from the LAS. Therefore, in first instance, the performance of ETLook at the point and at the catchment scale is checked by comparing the ETLook-results to daily averages of AE, H and LE from an EC-station in the catchment and to TOPLATS model results for the catchment.

As it seems that ETLook is able to estimate the energy balance terms for daily time steps at the point scale and at the catchment scale, it is used to validate the latent heat flux (or evapotranspiration rates) as estimated from the LAS and TOPLATS on a daily basis. As for the available energy, ETLook and the estimates from the Liedekerke point-measurements but adjusted to the catchment scale through the use of the hydrologic model show good correspondence. For the sensible and latent heat fluxes, daily averages show good correspondence between daily averages from LAS and ETLook-results, especially when daily averages from LAS-data are considered based on 24 available values of H and LE. Also, from the evapotranspiration rates calculated per 10-day period, there is a good correspondence between TOPLATS-results and both ETLook and LAS-derived evapotranspiration rates.

Consistency between hydrological model, LAS and remote sensing

B. Samain et al.

[Title Page](#)[Abstract](#)[Introduction](#)[Conclusions](#)[References](#)[Tables](#)[Figures](#)[◀](#)[▶](#)[Back](#)[Close](#)[Full Screen / Esc](#)[Printer-friendly Version](#)[Interactive Discussion](#)

References

Consistency between hydrological model, LAS and remote sensing

B. Samain et al.

[Title Page](#)

[Abstract](#)

[Introduction](#)

[Conclusions](#)

[References](#)

[Tables](#)

[Figures](#)

◀

▶

◀

▶

[Back](#)

[Close](#)

[Full Screen / Esc](#)

[Printer-friendly Version](#)

[Interactive Discussion](#)

Consistency between hydrological model, LAS and remote sensing

B. Samain et al.

Title Page	
Abstract	Introduction
Conclusions	References
Tables	Figures
◀	▶
◀	▶
Back	Close
Full Screen / Esc	
Printer-friendly Version	
Interactive Discussion	

- Kleissl, J., Watts, C. J., Rodriguez, J. C., Naif, S., and Vivoni, E. R.: Scintillometer intercomparison study-continued, *Bound.-Lay. Meteorol.*, 130, 437–443, doi:10.1007/s10546-009-9352-z, 2009b. 10867
- Kohsieck, W., Meijninger, W. M. L., Debruin, H. A. R., and Beyrich, F.: Saturation of the large aperture scintillometer, *Bound.-Lay. Meteorol.*, 121, 111–126, 2006. 10871
- 5 Mauder, M. and Foken, T.: Documentation and instruction manual of the eddy covariance software package TK2, Univ. of Bayreuth, Dept. of Mikrometeorology, Bayreuth, Germany, 2004. 10870
- Mauder, M., Foken, T., Clement, R., Elbers, J. A., Eugster, W., Grünwald, T., Heusinkveld, B., 10 and Kolle, O.: Quality control of CarboEurope flux data – Part 2: Inter-comparison of eddy-covariance software, *Biogeosciences*, 5, 451–462, doi:10.5194/bg-5-451-2008, 2008. 10870
- Meijninger, W., Hartogensis, O., Kohsieck, W., Hoedjes, J., Zurbier, R., and De Bruin, H. A. R.: Determination of area-averaged sensible heat fluxes with a large aperture scintillometer over 15 a heterogeneous surface – Flevoland field experiment, *Bound.-Lay. Meteorol.*, 105, 37–62, 2002. 10865
- Meijninger, W. M. L., Beyrich, F., Luedi, A., Kohsieck, W., and De Bruin, H. A. R.: Scintillometer-based turbulent fluxes of sensible and latent heat over a heterogeneous land surface – a contribution to LITFASS-2003, *Bound.-Lay. Meteorol.*, 121, 89–110, 2006. 10865
- Pauwels, V. and Samson, R.: Comparison of different methods to measure and model actual 20 evapotranspiration rates for a wet sloping grassland, *Agr. Water Manage.*, 82, 1–24, 2006. 10866, 10867
- Pelgrum, H., Miltenburg, I., Cheema, M., Klaasse, A., and Bastiaanssen, W.: ETLook a Novel Continental Evapotranspiration Algorithm, in: *Remote Sensing and Hydrology Symposium, Jackson Hole, Wyoming, USA*, 2010. 10875, 10876
- 25 Samain, B., Ferket, B., Defloor, W., and Pauwels, V.: Estimation of catchment averaged sensible heat fluxes sing a large aperture scintillometer, *Water Resour. Res.*, 47, W05536, doi:10.1029/2009WR009032, 2011a. 10867, 10868, 10870, 10871, 10872, 10873, 10878, 10879, 10881
- Samain, B., Defloor, W., and Pauwels, V.: Continuous time series of catchment-averaged sensible heat flux from a large aperture scintillometer: efficient estimation of stability conditions and importance of fluxes under stable conditions, *J. Hydrometeorol.*, accepted, 2011b. 30 10868, 10871, 10872, 10875, 10880, 10881

Consistency between hydrological model, LAS and remote sensing

B. Samain et al.

[Title Page](#)[Abstract](#)[Introduction](#)[Conclusions](#)[References](#)[Tables](#)[Figures](#)[◀](#)[▶](#)[◀](#)[▶](#)[Back](#)[Close](#)[Full Screen / Esc](#)[Printer-friendly Version](#)[Interactive Discussion](#)

Savage, M. J.: Estimation of evaporation using a dual-beam surface layer scintillometer and component energy balance measurements, *Agr. Forest Meteorol.*, 149, 501–517, doi:10.1016/j.agrformet.2008.09.012, 2009. 10866, 10867

Verstraeten, W. W., Veroustraete, F., and Feyen, J.: Assessment of evapotranspiration and soil moisture content across different scales of observation, *Sensors*, 8, 70–117, doi:10.3390/s8010070, 2008. 10865

Webb, E., Pearman, G., and Leuning, R.: Correction of flux measurements for density effects due to heat and water vapor transfer, *Q. J. Roy. Meteorol. Soc.*, 106, 85–100, 1980. 10870

Xu, C. and Singh, V.: Evaluation of three complementary relationship evapotranspiration models by water balance approach to estimate actual regional evapotranspiration in different climatic regions, *J. Hydrol.*, 308, 105–121, doi:10.1016/j.jhydrol.2004.10.024, 2005. 10865

5

10

Table 1. Input data for the three different techniques to calculate catchment averaged latent heat flux.

Parameter	Source	LAS	TOPLATS	ETLook
Temporal resolution: hourly or less				
LAS-intensities	LAS	x		
Air temperature	Liedekerke meteo-station	x	x	x
Air pressure	Liedekerke meteo-station	x		
Wind speed	Liedekerke meteo-station	x		x
Precipitation	Liedekerke meteo-station		x	x
Relative humidity	Liedekerke meteo-station		x	x
Net radiation	Liedekerke meteo-station	x	x	
Soil heat flux	Liedekerke meteo-station	x		
Temporal resolution: daily or more				
Surface albedo (resolution 30 m)	Satellite images (DMC, Landsat, ASTER)	x		
Normalized difference vegetation index (resolution 30 m)	Satellite images (DMC, Landsat, ASTER)	x		
Athmospheric transmissivity (resolution 6 km)	Meteosat Second Generation	x		
Maps				
Digital elevation model (DEM) (resolution 50 m)	Flanders Geographical Information Agency	x		
Soil texture map (resolution 50 m)	Flanders Geographical Information Agency	x		
Land cover map (resolution 50 m)	Flanders Geographical Information Agency	x		
Land cover map (resolution 30 m)	European Environment Agency		x	
Constants				
Effective height	Based on DEM (68 m)	x		
Zero-plane displacement height	Estimate (0.7 m)	x		
Surface roughness length	Estimate (0.3 m)	x		

Consistency between hydrological model, LAS and remote sensing

B. Samain et al.

[Title Page](#)

[Abstract](#)

[Introduction](#)

[Conclusions](#)

[References](#)

[Tables](#)

[Figures](#)

◀

▶

◀

▶

[Back](#)

[Close](#)

[Full Screen / Esc](#)

[Printer-friendly Version](#)

[Interactive Discussion](#)

Consistency between hydrological model, LAS and remote sensing

B. Samain et al.

[Title Page](#)

[Abstract](#)

[Introduction](#)

[Conclusions](#)

[References](#)

[Tables](#)

[Figures](#)

[◀](#)

[▶](#)

[◀](#)

[▶](#)

[Back](#)

[Close](#)

[Full Screen / Esc](#)

[Printer-friendly Version](#)

[Interactive Discussion](#)

Table 2. Statistics of the comparison between $\text{AE}_{\text{Liedekerke}}$ and $\langle \text{AE} \rangle_{\text{TOPLATS}}$ per month. Units are in W m^{-2} .

Month	$\text{AE}_{\text{Liedekerke}}$	$\langle \text{AE} \rangle_{\text{TOPLATS}}$	Slope	Intercept	R	RMSE	N
Jan	-2.75	-12.05	0.32	-11.16	0.67	29.35	2228
Feb	7.01	-6.73	0.48	-10.09	0.85	34.4	2206
Mar	33.68	17.25	0.64	-4.41	0.94	47.57	2966
Apr	68.23	54.27	0.74	3.95	0.98	46.03	2290
May	93.44	84.22	0.9	-0.29	0.98	33.7	2224
Jun	108.8	101.21	0.91	1.94	0.95	53.65	1640
Jul	105.82	99.52	0.92	1.9	0.97	39.73	2185
Aug	88.19	80.78	0.93	-1.14	0.99	25.35	2226
Sep	53.2	43.6	0.89	-3.67	0.98	26.18	2155
Oct	21.72	10.27	0.63	-3.44	0.94	35.36	2226
Nov	-0.93	-16.34	0.43	-15.94	0.78	31.16	2155
Dec	-5	-15.2	0.24	-13.98	0.52	27.22	2222

Consistency between hydrological model, LAS and remote sensing

B. Samain et al.

[Title Page](#)

[Abstract](#)

[Introduction](#)

[Conclusions](#)

[References](#)

[Tables](#)

[Figures](#)

◀

▶

◀

▶

[Back](#)

[Close](#)

[Full Screen / Esc](#)

[Printer-friendly Version](#)

[Interactive Discussion](#)

Table 3. Evapotranspiration sums for every 10-day period in the considered six months period from estimates by ETLook, TOPLATS and LAS. Only days where 24 hourly data from LAS are available are considered. The number of considered days within the 10-day period is indicated by N .

Year	Month	Days for 10-day period	N (days)	ETLook (mm)	TOPLATS (mm)	LAS (mm)
2009	Apr	1–10	3	4.78	3.88	2.96
		11–20	3	6.12	4.92	2.63
		21–30	5	8.02	8.29	4.72
	May	1–10	8	12.78	15.98	12.09
		11–20	8	13.67	16.70	13.48
		21–31	8	21.41	23.91	20.09
	Jun	1–10	8	16.52	19.13	15.54
		11–20	0	—	—	—
		21–30	0	—	—	—
	Jul	1–10	7	14.93	17.98	14.96
		11–20	4	10.11	11.28	12.03
		21–31	8	24.53	22.89	23.28
	Aug	1–10	6	19.10	18.43	18.70
		11–20	5	12.07	12.71	12.73
		21–31	9	22.17	20.23	17.21
	Sep	1–10	10	17.28	16.74	12.37
		11–20	4	5.78	4.25	3.02
		21–30	3	3.56	2.90	0.77

Consistency between hydrological model, LAS and remote sensing

B. Samain et al.

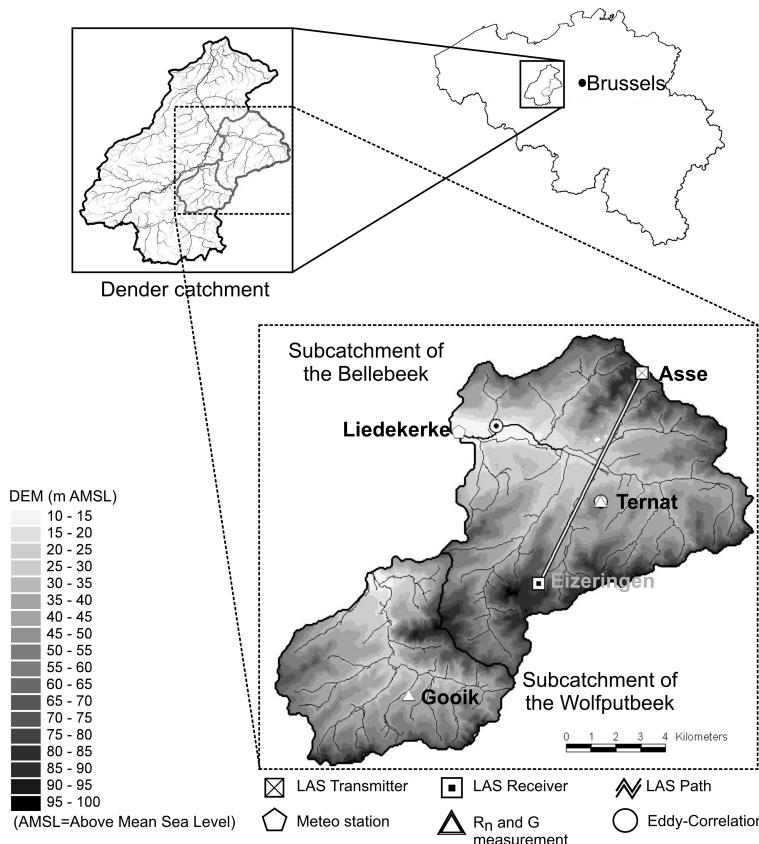


Fig. 1. The location of the study site in Belgium, a DEM of the study area and the location of the meteorologic stations and the LAS in the study area.

Consistency between hydrological model, LAS and remote sensing

B. Samain et al.

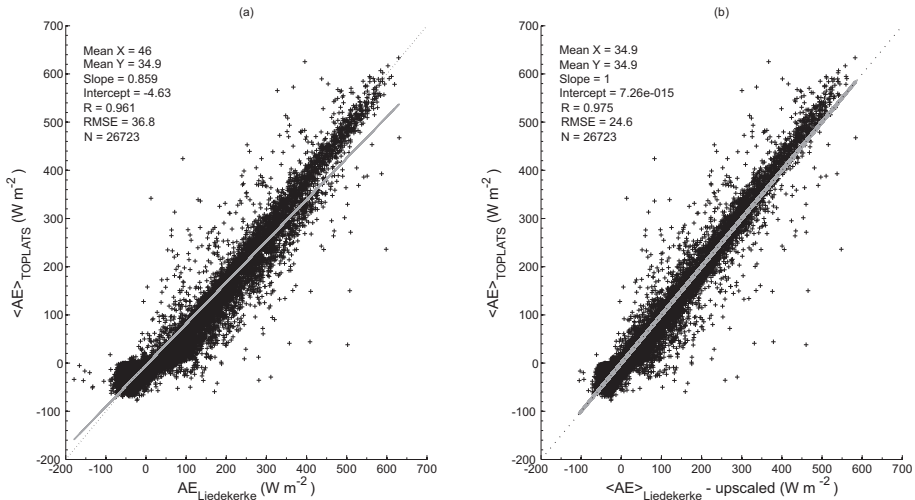


Fig. 2. Comparison between $\text{AE}_{\text{Liedekerke}}$ and $\langle \text{AE} \rangle_{\text{TOPLATS}}$ (a) and comparison between upscaled values of $\text{AE}_{\text{Liedekerke}}$ for the catchment according to the monthly statistics as given in Table 2 (b).

Title Page

Abstract

Introduction

Conclusions

References

Tables

Figures

◀

▶

◀

▶

Back

Close

Full Screen / Esc

Printer-friendly Version

Interactive Discussion

Consistency between hydrological model, LAS and remote sensing

B. Samain et al.

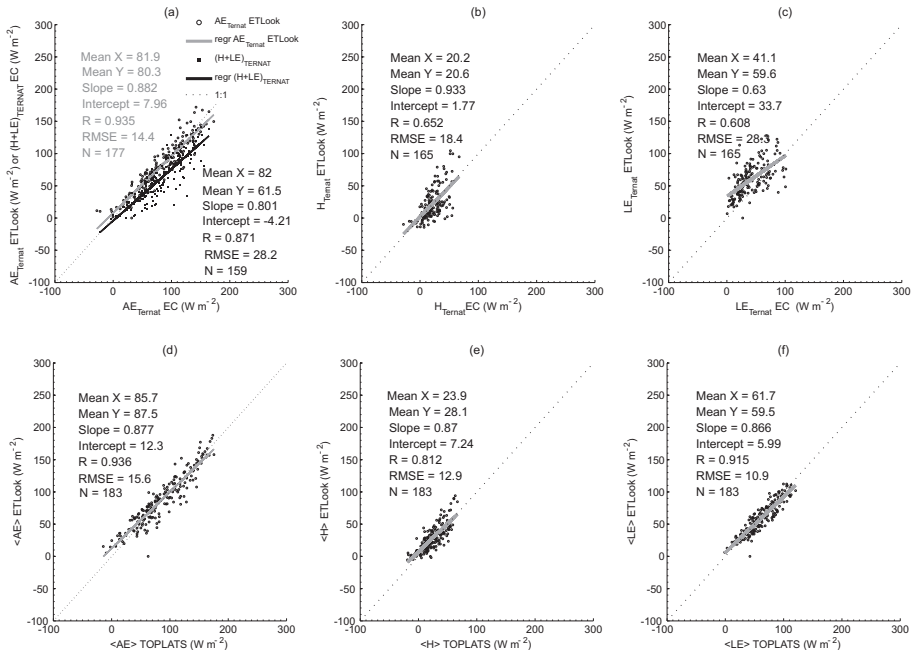


Fig. 3. Comparison for AE, H and LE between ETLook and point-measurements (**a–c**), and between ETLook and TOPLATS (**d–f**).

Consistency between hydrological model, LAS and remote sensing

B. Samain et al.

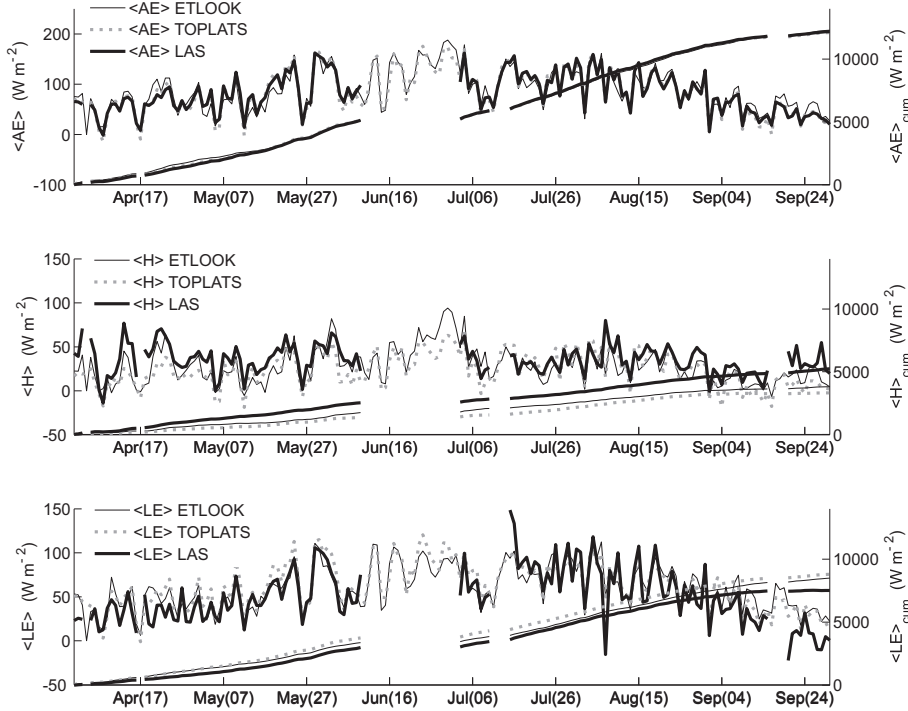


Fig. 4. Timeseries for daily $\langle AE \rangle$ (top), $\langle H \rangle$ (middle) and $\langle LE \rangle$ (bottom) as calculated by ETLook, TOPLATS and LAS for the Bellebeek catchment. Cumulative values for the available days are given as well (right axes).

Consistency between hydrological model, LAS and remote sensing

B. Samain et al.

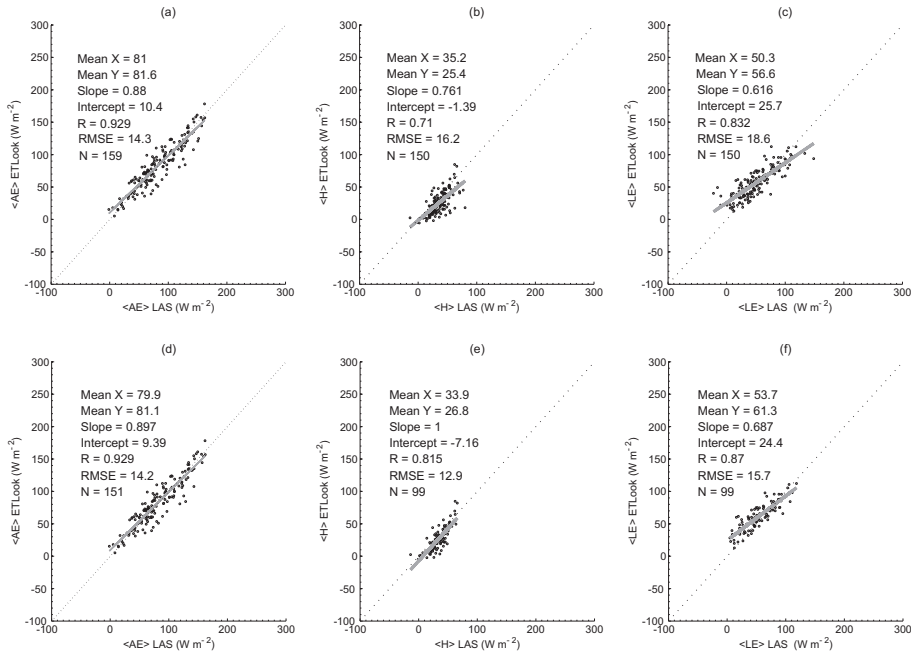


Fig. 5. Comparison for ETLook-derived and LAS-derived AE, H and LE for days where for at least 12 h LAS-data are available (**a–c**), and for days where all 24 h are available for LAS (**d–f**).

[Title Page](#)

[Abstract](#)

[Introduction](#)

[Conclusions](#)

[References](#)

[Tables](#)

[Figures](#)

◀

▶

◀

▶

[Back](#)

[Close](#)

[Full Screen / Esc](#)

[Printer-friendly Version](#)

[Interactive Discussion](#)